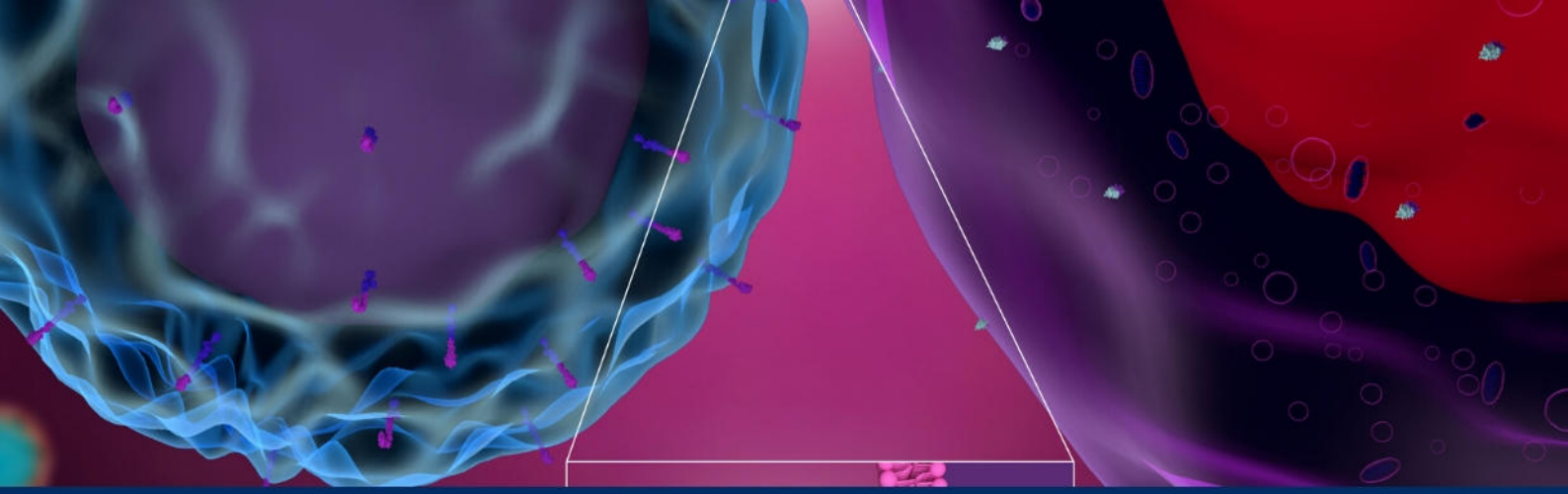

Applications in CAR T-cell Therapy: Dissecting Cellular Composition Using Single Cell Multiomics

Tuesday, March 24th (US)
5:00pm EST, 2:00pm PST
Wednesday, March 25th (AU)
8:00am NSW

Free Webinar
Register Now

Sponsored by

BD

Provided by

CURRENT PROTOCOLS
A Wiley Brand

WILEY

IJC
International Journal of Cancer

Circulating *cKIT* and *PDGFRA* DNA indicates disease activity in Gastrointestinal Stromal Tumor (GIST)

Stefanie Jilg[1]*, Michael Rassner[2]*, Jacqueline Maier[3], Silvia Waldeck[2,4,5], Victoria Kehl[6], Marie Follo[2], Ulrike Philipp[2], Andreas Sauter[7], Katja Specht[8], Jan Mitschke[2,4], Thoralf Lange[9], Sebastian Bauer[10], Philipp J. Jost[1], Christian Peschel[1], Justus Duyster[2,4], Timo Gaiser[11], Peter Hohenberger[12] and Nikolas von Bubnoff[2,4,13]

[1]III Medical Department for Hematology and Oncology, Klinikum Rechts der Isar, Technische Universität München, Munich, Germany
[2]Department of Hematology, Oncology and Stem Cell Transplantation, Medical Center, Faculty of Medicine, University of Freiburg, Freiburg, Germany
[3]Center for Internal Medicine, Department of Hematology/Oncology and Hemostaseology, University of Leipzig, Leipzig, Germany
[4]German Cancer Consortium (DKTK) partner site Freiburg and German Cancer Research Center (DKFZ), Heidelberg, Germany
[5]Faculty of Biology, University of Freiburg, Freiburg, Germany
[6]Institute for Medical Informatics, Statistics, and Epidemiology, Klinikum Rechts der Isar, Technische Universität München, Munich, Germany
[7]Department of Diagnostic and Interventional Radiology, Klinikum Rechts der Isar, Technische Universität München, Munich, Germany
[8]Institute of Pathology, Klinikum Rechts der Isar, Technische Universität München, Munich, Germany
[9]Asklepios Klinik Weißenfels, Weißenfels, Germany
[10]Sarcoma Center, West German Cancer Center, University Hospital Essen, University Duisburg-Essen, Essen, Germany
[11]Institute of Pathology, University Medical Center Mannheim, Ruprecht-Karl University of Heidelberg, Mannheim, Germany
[12]Division of Surgical Oncology and Thoracic Surgery, University Medical Center Mannheim, Ruprecht-Karl University of Heidelberg, Mannheim, Germany
[13]Department of Hematology and Oncology, Medical Center, University of Schleswig Holstein, Lübeck, Germany

This prospective trial aimed to investigate whether tumor-specific *cKIT* and *PDGFRA* mutations can be detected and quantified in circulating tumor (ct)DNA in patients with active GIST, and whether detection indicates disease activity. We included 25 patients with active disease and *cKIT* or *PDGFRA* mutations detected in tissue. Mutant ctDNA was detected in the peripheral blood plasma using allele-specific ligation (L-)PCR and droplet digital (d)PCR. CtDNA harboring tumor-specific *cKIT* or *PDGFRA* mutations was detected at least once in 16 out of 25 patients using L-PCR (64%) and in 20 out of 25 patients with dPCR (80%). Using dPCR, the absolute numbers of ctDNA fragments (DNA copies/ml) and the mutant allele frequency (MAF; in percent of wild-type control) strongly correlated with tumor size expressed as RECIST1.1 sum of diameter (SOD) in mm (ρ = 0.3719 and 0.408, respectively, $p < 0.0001$) and response status (ρ = 0.3939 and 0.392, respectively, $p < 0.0001$ and $p < 0.001$). Specificity of dPCR for detection of progression was 79.2% with a sensitivity of 55.2% and dPCR discriminated CR from active disease with a specificity of 96% and s sensitivity of 44.7%. With L-PCR, correlations of MAF with tumor size and response status were less prominent. Serial ctDNA measurement reflected individual disease courses over time. Targeted panel sequencing of four patients detected additional driver mutations in all cases and secondary resistance mutations in two cases. Thus, ctDNA indicates disease activity in patients with GIST and should be incorporated as companion biomarker in future prospective trials.

Key words: liquid biopsy, circulating tumor DNA, GIST, cancer biomarker

Abbreviations: CR: complete response; cKIT: v-kit Hardy–Zuckerman 4 feline sarcoma viral oncogene homolog; ctDNA: circulating tumor DNA; dPCR: droplet digital polymerase chain reaction; GIST: Gastrointestinal Stromal Tumor; ITT: intention to treat; L-PCR: ligation-polymerase chain reaction; MAF: mutant allele frequency; PD: progressive disease; PDGFRA: platelet-derived growth factor receptor-alpha; PFS: progression-free survival; PR: partial response; RECIST: response evaluation criteria in solid tumors; SD: stable disease; SOD: sum of diameter; TKI: tyrosine kinase inhibitor

Additional Supporting Information may be found in the online version of this article.

Conflict of interest: NvB received honoraria from Astra Zeneca, Amgen, Novartis and BMS and research funding from Novartis. The other authors have no conflicts of interest to disclose.

*S.J. and M.R. contributed equally to this work

Grant sponsor: Bundesministerium für Bildung und Forschung; **Grant number:** 13GW0198E; **Grant sponsor:** German Cancer Consortium (DKTK); **Grant number:** L665; **Grant sponsor:** Novartis Pharma; **Grant number:** CSTI5781BDE78T; **Grant sponsor:** Comprehensive Cancer Center Freiburg (CCCF); **Grant sponsor:** University of Freiburg Medical Faculty

DOI: 10.1002/ijc.32282

History: Received 9 Aug 2018; Accepted 5 Mar 2019; Online 18 Mar 2019.

Correspondence to: Nikolas von Bubnoff, MD, Department of Hematology and Oncology, Medical Center, University of Schleswig Holstein, Campus Lübeck, Ratzeburger Allee 160, 23538 Lübeck, Germany, Tel.: +49-451-500-44150, Fax: +49-451-500-44154, E-mail: nikolas.von.bubnoff@outlook.de

What's new?

For Gastrointestinal Stromal Tumors (GIST), early detection of relapsed or progressive disease is mandatory to provide adequate surgical procedures or switch medication in case of drug resistance. However, until now monitoring of GIST patients has been restricted to imaging with technical limits in sensitivity and specificity, calling for biomarkers to be developed. In this prospective trial, the authors demonstrate that in GIST patients, the amount of circulating tumor (ct)DNA harboring tumor-specific cKIT and PDGFRA mutations correlates with disease activity and tumor size. Thus, analysis of ctDNA might complement standard imaging techniques for monitoring and follow-up in GIST.

Introduction

Gastrointestinal Stromal Tumors (GIST) are the most common mesenchymal tumors of the gastrointestinal tract with an incidence rate of 1–2 cases/100,000/year.[1,2] Complete surgical resection is the only curative treatment.[3] In patients with metastatic GIST, the median progression-free survival (PFS) in patients receiving imatinib is 18–24 months[4] with 35% of the patients surviving after 9 years of imatinib treatment.[5] Novel tyrosine kinase inhibitors (TKI) like sunitinib or regorafenib have allowed sequential treatments and thus substantially improved the survival of patients with metastatic GIST.[6] After failure of imatinib, half of the patients benefit from a change to second-line sunitinib.[7] Ongoing clinical trials investigate the clinical activity of novel inhibitors such as ponatinib (POETIG/NCT03171389), cabozantinib (CABOGIST/NCT02216578), avapritinib (NCT02508532) or DCC-2618 (NCT02571036) in case of failure of standard therapy.

In patients with localized GIST, the recurrence-free survival after surgery without adjuvant treatment is 57.3% after 20 years.[8] Thus, more than 40% of patients could potentially benefit from adjuvant treatment. Tumor size, localization, mitotic index and tumor rupture are associated with increased risk of relapse.[9–11] Although adjuvant treatment improves recurrence-free survival in patients with high risk of relapse, a proportion of patients will ultimately relapse after cessation of adjuvant treatment.[12]

Early detection of relapsed or progressive disease is mandatory to provide adequate surgical procedures or to switch medication in case of TKI resistance. However, until now monitoring of GIST patients is restricted to imaging. Current imaging techniques are limited in sensitivity and specificity[13–15] and specific protein biomarkers do not exist. Thus, biomarkers to identify patients at risk of relapse during adjuvant or palliative treatment are urgently needed.

In 85–90% of cases, GIST tumors harbor a tumor-specific v-kit Hardy–Zuckerman 4 feline sarcoma viral oncogene homolog (cKIT) or platelet-derived growth factor receptor-α (PDGFRA) mutation.[11,16] We have shown previously that circulating, tumor-derived DNA fragments (ctDNA) carry the individual mutation in *cKIT* or *PDGFRA*.[17] These mutated genomic DNA fragments are tumor specific. Allele-specific polymerase chain reaction (PCR) allows specific amplification and quantification of the mutated *cKIT* and *PDGFRA* DNA fragments with high sensitivity. We therefore reasoned that the presence and amount of genomic tumor DNA in plasma samples harboring GIST-specific mutations might be used as biomarker in patients with GIST. The *CF*-DNA GIST trial was designed as multicenter, prospective, explorative and phase IIIb trial. The main objective was to investigate whether tumor-specific *cKIT* or PDGFRA ctDNA fragments can be detected and quantified in the plasma of patients with active GIST. CtDNA was measured by ligation PCR (L-PCR) and droplet digital (d) PCR. In selected cases, targeted next-generation sequencing (NGS) was performed. Detection of ctDNA in the peripheral blood and ctDNA amount were correlated with disease activity and the course of disease.

Materials and Methods

Study design

Our study was designed as an open-label, nonrandomized, noninterventional, prospective, explorative, multicenter phase IIIb trial for the detection of circulating cell-free tumor DNA in the plasma of patients with active GIST harboring activating mutations of *cKIT* or *PDGFRA*. Patients with at least one GIST lesion (measurable by CT, PET-CT or MRI) were included in case of planned surgery of one or more disease manifestations or planned TKI treatment in neoadjuvant or palliative intention, or disease progression irrespective of current/planned treatment (Supporting Information Table S1). Patients were excluded in case of completed surgery without evidence of progressive lesions, adjuvant TKI treatment after surgery and no evidence of progressive lesions or palliative TKI treatment and no evidence of progressive lesions. For each individual patient, DNA fragments carrying mutated *cKIT* or *PDGFRA* released by the tumor were amplified and quantified by allele-specific PCR every 3 months over a period of 2 years. The levels of ctDNA were correlated with the clinical course of disease. Based on the binomial distribution, a sample size of 25 patients was suspected to result in a 95% CI for the proportion of patients with successful detection (primary endpoint), stretching 20% on both sides of the observed percentage. The full study protocol is provided in the Supporting Information section.

Primary endpoint was the percentage of patients with histologically proven GIST, measurable lesion in imaging and activating *cKIT* and *PDGFRA* mutation detectable in ctDNA by L-PCR or dPCR at least at one-time point. Secondary endpoints included the correlation between the amount of tumor-specific *cKIT* or PDGFRA DNA in plasma samples and the amount of tumor as assessed by

diagnostic imaging, response to therapy (surgery and/or therapy with a TKI) or relapse or progression of the disease as assessed by diagnostic imaging. Furthermore, the sensitivity of L-PCR and dPCR for specific *cKIT* or *PGDFRA* mutations was analyzed. The study was approved by the responsible Institutional Review Board (Technical University of Munich, 5108/11). This trial was registered under Eudra-CTNo. 2011-002544-27 and ClinicalTrials.gov NCT01462994. This trial received financial support by Novartis Pharma (Study Code: CSTI571BDE78T).

Patients

From January 2012 (first patient, first visit) to October 2015 (last patient, last visit), a total of 35 patients with active GIST were enrolled at five participating centers throughout Germany. All subjects provided written informed consent before enrollment. The study was conducted in accordance with Good Clinical Practice and the Declaration of Helsinki. All authors vouched for the accuracy and completeness of the reported data, analyses and the adherence of the study protocol.

Eligible patients were aged ≥18 years, had a life expectancy of at least 3 months, a histologically confirmed GIST with proven mutation in *cKIT* or *PDGFRA*, a measurable lesion at baseline imaging and sufficient tissue available for baseline mutational analysis (Supporting Information Table S1). Patients underwent routinely planned follow-up visits in 3 months intervals with local standard of care diagnostic imaging (CT, PET-CT or MRI). Baseline characteristics are shown in Table 1, detailed previous medical history of all patients is shown in Supporting Information Table S2.

Specimen characteristics

Serial plasma samples (n = 156) were collected from 25 patients with active GIST and activating mutations in *cKIT* or *PDGFRA*. Blood samples were taken at baseline and at routine follow-up visits in 3 months intervals for a period of up to 2 years.

Assay methods

Mutation analysis of DNA from tumor tissue. A tumor-specific mutation site of each subject was determined by Sanger sequencing of genomic DNA extracted from tumor tissue as described previously.[17]

Sample processing. Circulating cell-free DNA was isolated from 18 ml of peripheral blood at each visit. Peripheral blood samples were collected in EDTA tubes (Sarstedt, Nümbrecht, Germany). Up to 4 hr after blood withdrawal, collection tubes were centrifuged at 800 *g* for 10 min. The supernatant was transferred to 10 ml tubes and centrifuged at 1,600 *g* for 10 min to remove debris. Plasma supernatants were stored at −80°C. Total genomic DNA of plasma aliquots were extracted from 1 ml plasma using the QIAamp Circulating Nucleic Acid Kit (Qiagen, Hilden, Germany) according to the manufacturer's instructions. Isolated DNA was stored at −20°C. When using plasma probes from healthy controls, the material was processed likewise.

Table 1. Baseline characteristics

Total, *n*	25
Sex, *n* (%)	
Male	13 (52%)
Female	12 (48%)
Median age, years (range)	60.9 (34–81)
Tumor-specific mutation, *n* (%)	25 (100%)
KIT exon 9 A502-Y503dup	2 (8%)
KIT exon 11 K550-E554del	1 (4%)
KIT exon 11 P551-E554del	1 (4%)
KIT exon 11 P551-K558del InsQ	1 (4%)
KIT exon 11 Y553-Q556del	1 (4%)
KIT exon 11 E554-W557del InsV	1 (4%)
KIT exon 11 V555-D572del InsG	1 (4%)
KIT exon 11 Q556-V560del InsH	1 (4%)
KIT exon 11 W557-K558del	2 (8%)
KIT exon 11 W557R/G	2 (8%)
KIT exon 11 W557-V560del InsF	1 (4%)
KIT exon 11 V559D	1 (4%)
KIT exon 11 V559G	1 (4%)
KIT exon 11 V559A	1 (4%)
KIT exon 11 V560D	2 (8%)
KIT exon 11 I563-T574del	1 (4%)
KIT exon 11 L576P	1 (4%)
KIT exon 11 P577del	1 (4%)
KIT exon 11 D579del	1 (4%)
KIT exon 17 D820G	1 (4%)
PDGFRA exon 18 D842V	1 (4%)
PDGFRA exon 18 D842-H845del	1 (4%)
Stage at baseline	
Localized, *n* (%)	8 (32%)
Primary diagnosis, *n* (%)	5 (20%)
Stomach	4 (16%)
Rectum	1 (4%)
Relapse, *n* (%)	3 (12%)
Stomach	1 (4%)
Intestine	1 (4%)
Liver	1 (4%)
Metastatic, *n* (%)	17 (68%)
Primary diagnosis, *n* (%)	4 (16%)
Relapse, *n* (%)	13 (52%)
Previous therapy (medical and/or surgery), *n* (%)	17 (68%)
TKI treatment, *n* (%)	14 (56%)
>1 line of treatment, *n* (%)	6 (24%)
Surgery, *n* (%)	16 (64%)
>1 surgery, *n* (%)	8 (32%)
Treatment with TKI at baseline, *n* (%)	9 (36%)
Imatinib	5 (20%)
Sunitinib	3 (12%)
Sorafenib	1 (4%)

Baseline characteristics of the study population are provided including sex, age, tumor-specific mutation, stage of GIST at baseline (localized *vs*. metastatic) and previous therapy including surgery and treatment with tyrosine kinase inhibitors (TKI).

Ligation PCR. L-PCR was performed as previously described.[17] Sensitivity of L-PCR has been tested for cloned key mutations (including *cKIT* exon 9 insertion 502–503; *cKIT* exon 11 deletion 557–558; *cKIT* exon 11 V559D; *PDGFRA* exon 18 D842V) and ranged from 0.01% to 0.1% (mutated allele/unmutated allele) dependent on cross-reactivity of hybridizing probes. This resulted in a dynamic detection range of 4–5 log10. Cross-reactivity was analyzed for each assay using healthy controls (negative controls) and the nonspecific allelic level (background) was subtracted from the positive allelic level of the patient samples.

Droplet digital PCR. For dPCR, 16 customized assays were designed and validated. Primer pairs and locked nucleic acid (LNA) or standard-probes for wild-type or mutation were designed using Beacon Designer (Merck, Darmstadt, Germany) avoiding primer pairing. Primers were manufactured by IDT DNA Technologies (Coralville, IA). Fluorescein (FAM)- or hexafluorescein (HEX)-labeled mutant or wild-type probes were either LNA or standard probes (Supporting Information Table S3). Temperature gradients PCR and DNA dilutions assays of decreasing mutant allele (MAF) frequency were conducted to determine optimal conditions for each assay and to test for analytical sensitivity.

For each dPCR, 11 µl Supermix (Bio-Rad Laboratories GmbH, Munich, Germany) was added to 0.22 µl primers (forward and reverse), 1.1 µl probes and 7 µl DNA eluate. Molecular H_2O was added to obtain 22 µl mix. Twenty microliters were used for each well. All measurements were conducted at least in quadruplets and the mean was used for analysis. The droplets were generated in the Automated Droplet Generator (Bio-Rad Laboratories GmbH, Munich, Germany). Subsequently, the obtained droplets were cycled (C1000 Touch™ Thermal Cycler, Bio-Rad Laboratories GmbH, Munich, Germany) with the following cycling steps: (*i*). 10 min at 95°C, (*ii*) 40 cycles of 30 sec at 95°C followed by 1–2 min at the predetermined optimal T° and (*iii*) 10 min at 98°C. Finally, the droplet fluorescence was measured in the QX 200™ Droplet Reader (Bio-Rad Laboratories GmbH, Munich, Germany). Data were analyzed using the QuantaSoft software (Bio-Rad Laboratories GmbH, Munich, Germany). Controls were analyzed concurrently that included wild-type DNA or no DNA. Limit of blank (LOB) values were determined for each assay in plasma probes from healthy controls and LOB was subtracted from results. Limit of detection values were determined for each assay using dilution series of mutant DNA spiked into wt DNA (Supporting Information Table S3).

Next-generation sequencing

CfDNA isolated from blood plasma was concentrated by SpeedVac (Thermo Fisher Scientific, Waltham, MA) followed by quality control with Fragment Analyzer (Agilent Technologies, Santa Clara, CA) and quantification by Qubit 2.0 fluorometer (Thermo Fisher Scientific, Waltham, MA). Libraries were prepared using 5–25 ng of DNA according to the manufacturer's instructions using the molecular-barcode/Unique identifier (UID) containing ThruPlex Tag-Seq 48S Kit (Takara, Kusatsu, Japan). Clean-up and size-selection of the library products was conducted using AMPure XP beads (Beckman Coulter, Brea, CA). Quality was controlled with Fragment Analyzer and the concentration of the libraries was quantified by Qubit 2.0 fluorometer. Target enrichment was performed using a custom probe panel (Integrated DNA Technologies, Coralville, IA) according to manufacturer's instructions The following 18 genes were selected in the custom IDT panel: *BRAF* (exons 11, 15), *CDKN2A* (exons 1, 2), *CTNNB1* (exon 3), *EGFR* (exons 18, 19, 20, 21), *HER2/ERBB* (exon 20), *HRAS* (exons 2, 3), *KEAP1* (exons 2, 3, 4, 5, 6), *KIT* (9, 11, 13, 14, 17), *KRAS* (2, 3, 4), *MET* (exon 14), *NFE2L2* (exon 2), *NRAS* (exons 2, 3), *PDGFRA* (exon 18), *PIK3CA* (exons 10, 21), *PTEN* (exons 1, 3, 6, 7, 8), *SDHA* (exons 2, 7, 13), *SMAD4* (1, 2, 8, 9, 10, 11), *TP53* (exons 4, 5, 6, 7, 8, 9, 10). The captured libraries were size-selected and purified with AMPure XP beads. The concentration of the postcapture products and the multiplex-NGS pool was determined *via* qPCR (lightcycler Rotor-Gene Q, Qiagen, Hilden, Germany) by use of the KAPA Library Quantification Kit (Roche, Basel, Switzerland). Paired-end sequencing of the multiplex-NGS pool was performed by "Genomics and Proteomics Core Facility" of the DKFZ Heidelberg (Germany) on a HiSeq 2000 (Illumina, San Diego, CA). Sensitivity of the combined UID-target capture NGS Panel was tested using diluted sheared genomic DNA that harbored known mutations as well as the "Cell-Free DNA Reference Standard Set" (Horizon Discovery, Waterbeach, UK), which contains single nucleotide variants (SNVs/SNPs) of eight mutations at known allele frequencies.

Sequence data analysis

The obtained FASTQ-files were mapped to the human genome (hg19) with BWA and demultiplexed with Connor. Grouping of molecular barcode/unique identifier (UID) families was performed using SamTools. Read ends were trimmed (18 bp) with TrimGalore. Mutation calling of the resulting data was done with the software Sequence Pilot (JSI medical systems GmbH, Ettenheim, Germany).

Statistical analysis methods

The amount of tumor as assessed at each visit by diagnostic imaging was computed as the sum of the lengths of all lesions (maximum 5 per imaging, response evaluation criteria in solid tumors [RECIST] 1.1 criteria, central assessment used where available). The response to therapy as assessed by diagnostic imaging could take the following values: complete response (CR), partial response (PR), stable disease (SD); nonresponse to therapy was defined as local progression (LP) or progressive disease (PD). All nonmissing data were included in the analysis with the exception of missing tumor size when response was CR. These were imputed with 0, as obviously no tumor was present. Correlation between the amount of ctDNA and a number of clinical variables like amount of tumor or response to therapy was performed using Spearman's ρ correlation coefficient. Differences in the amount of ctDNA measured for

patients with response (CR, PR and SD) and progression (PD) were tested with the Mann–Whitney U test.

Results

Thirty-five patients with active GIST and known activating mutation in the c*KIT* or *PDGFRA* gene were screened. Ten patients had to be excluded from the intention to treat analysis due to screening failure (Fig. 1). Twenty-five patients were included in the intention to treat analysis set, 12 females and 13 males. Patient characteristics are shown in Table 1. The age ranged between 34 and 81 with a median of 60.9 years. Eight patients (32%) had localized GIST and 17 patients (68%) metastatic disease. Previous therapy in 17 patients (68%) contained medical treatment with TKI in 14 patients (56%) including 6 patients (24%) with more than one line of treatment, and surgery in 16 patients (64%), including 8 patients (32%) who had received more than one surgical intervention. Of note, nine patients at the time of inclusion received medical treatment, five imatinib, three sunitinib and one sorafenib, respectively (Table 1).

Individual characteristics of the disease and treatments are shown in Supporting Information Table S2. In line with published reports, most individuals (84%) had a mutation in *cKIT* exon 11 (21 out of 25; Table 1 and Supporting Information Table S2). In one individual, a mutation in *cKIT* exon 11, V555-D572del InsG, as well as a mutation in *cKIT* exon 17, D820G, was detected at baseline. Two patients (8%) carried a mutation in exon 9 (A502-Y503dup) and two had a *PDGFRA* mutation (8%; Supporting Information Table S2). GIST-specific treatment after inclusion was given according to Investigator's Choice. Thirteen patients (52%) underwent surgery during the course of the study and four patients had repeated surgical interventions. Twenty of 25 patients (80%) received at least one TKI during the course of the study, 10 patients (40%) were treated with more than one TKI (Supporting Information Table S2). The median follow-up time was 22 months. Three patients (12%) died during the course of the study and six patients (24%) were lost to follow-up with a median time until lost to follow-up of 10 months (Fig. 1).

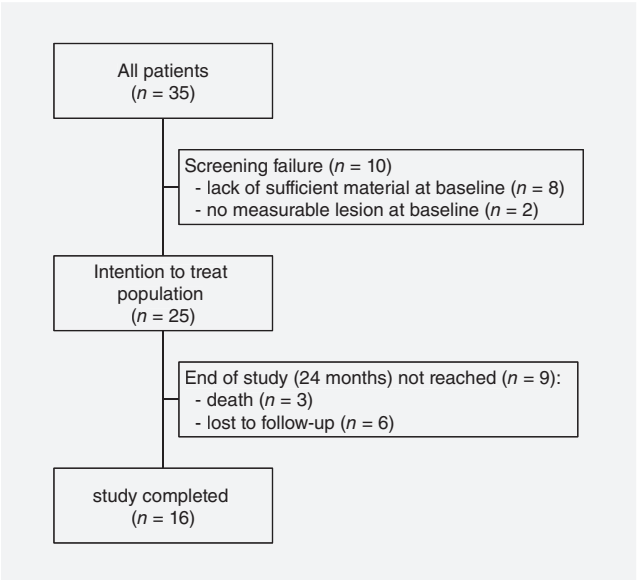

Figure 1. Trial profile. Thirty-five patients with active GIST were screened for ctDNA. Ten patients were identified as screening failure, 25 were included in the intention to treat population. Thereof, 16 individuals (64%) completed the study, three died during the course of the study and six were lost to follow-up.

Successful detection of ctDNA in patients with active GIST and known mutations in *cKIT or PDGFRA*

In 25 patients with GIST and at least one measurable lesion, we aimed to determine whether mutations in the c*KIT* or *PDGFRA* gene detected in tissue specimens can be recovered in ctDNA isolated from plasma samples. For these 25 patients, 156 plasma samples were collected and analyzed for the presence of ctDNA (Supporting Information Table S4). Using L-PCR, 16 of 25 patients in the ITT set were positive for tumor-specific DNA in the plasma at least once, giving a detection rate in the primary endpoint of 64% with L-PCR, in line with our previous data.[17] Eight (50%) of the L-PCR positive patients had progressive disease at the time of positive sample. Using dPCR, ctDNA encoding for mutated c*KIT* or *PDGFA* was detected at least once during the course of the study in 20 out of 25 patients (80%). Combining dPCR with L-PCR, ctDNA was detected in 23 out of 25 patients (92%). One patient lacking detectable ctDNA had a mutation in exon 11 (P551-E554del) and a single small intestine lesion measuring 0.51 cm that was slightly progressive to a size of 0.63 cm while receiving pazopanib. The second patient with negative ctDNA test had a P577del in exon 11 and had gastric and peritoneal lesions. The patient responded to imatinib treatment and had achieved PR at inclusion.

Thus, ctDNA harboring activating *cKIT* or *PDGFRA* mutations was successfully detected in 92% of patients with active GIST. Use of dPCR significantly increased the detection rate compared to L-PCR.

The amount of tumor-specific ctDNA correlates with tumor size

We next asked whether ctDNA levels correlated with the radiologically determined extent of tumor, expressed as RECIST1.1 sum of diameter (SOD) in mm. The amount of ctDNA fragments was either determined as absolute number (DNA copies/ml; dPCR) or as mutant allele frequency (MAF) in percent of wild-type control.

Using dPCR, the absolute numbers of ctDNA fragments (DNA copies/ml, Fig. 2*a*) and the MAF in percent of wt (Fig. 2*b*) correlated with tumor size (Spearman's correlation coefficient $\rho = 0.3719$; $p < 0.001$ and $\rho = 0.408$; $p < 0.0001$, respectively). The abundance of ctDNA measured by dPCR correlated with MAF values measured by L-PCR (Figs. 2*c* and 2*d*). However, only the analysis of samples from patients with at least one positive value showed a statistically significant correlation ($p = 0.0326$). Using L-PCR, a positive correlation between ctDNA MFA and tumor

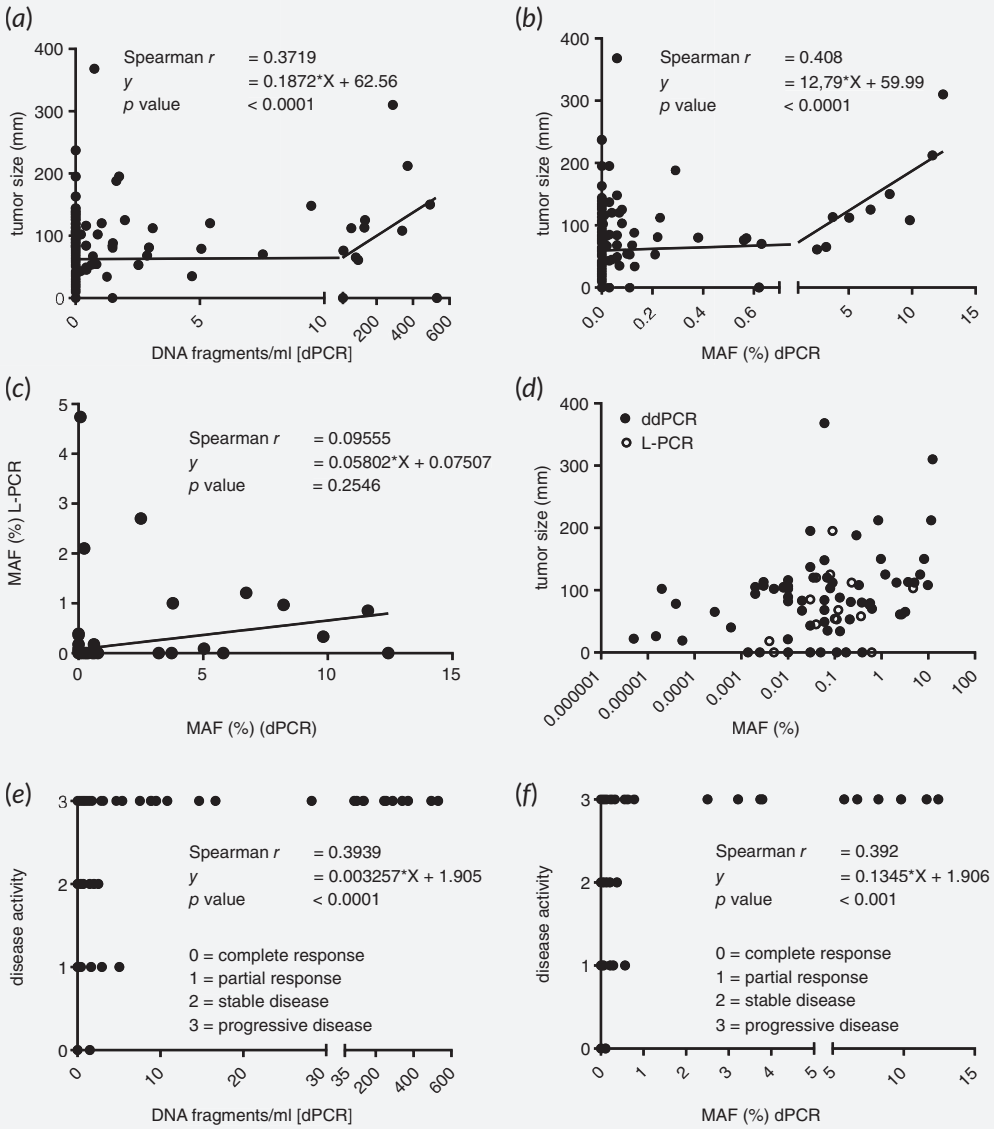

Figure 2. Amount of tumor-specific ctDNA measured by dPCR positively correlates with disease activity and tumor size. Circulating tumor DNA (ctDNA) was measured by ligation PCR (L-PCR) or digital droplet PCR (dPCR) and compared to wild-type (wt) control. MAF is shown in percentage of wild-type control. (*a*) The absolute copy number (DNA fragments/ml) of each sample measured by dPCR or (*b*) the mutant allelic frequency (MAF in % total control) was plotted against tumor size, expressed as RECIST1.1 sum of diameter (SOD) in mm. The strength of the association between ctDNA value and tumor size was calculated by the Spearman rank correlation and the functional relationship was described by linear regression analysis. (*c*) For each sample, the MAF value (% total control) measured by dPCR was compared to the corresponding MAF values (% total control) measured by L-PCR. (*d*) The MAF (% total control) of each sample was plotted against tumor size (mm). Filled circles indicate values measured by dPCR, open circles indicate values measured by L-PCR. (*e*) The absolute copy number (DNA fragments/ml) of each sample measured by dPCR or (*f*) the MAF (% total control) was plotted against tumor activity as indicated. Tumor activity was determined by standard imaging techniques using response evaluation criteria in solid tumors (RECIST, version 1.1). The strength of the association between ctDNA value and tumor size was calculated by the Spearman rank correlation and the functional relationship was described by linear regression analysis.

size was detected ($\rho = 0.09772$; $p = 0.2769$; Supporting Information Fig. S1A and S1B). In patients with detectable cfDNA at baseline, the correlation was statistically significant ($\rho = 0.32$; $p = 0.044$).

Taken together, the absolute number of cfDNA fragments in the plasma and the fraction relative to wild-type (MAF) reflects the tumor burden of patients with GIST and dPCR seemed to more accurately reflect the amount of tumor.

CtDNA levels in GIST patients indicate response status

In order to determine whether ctDNA is informative with regard to disease activity, the amount of mutant ctDNA was correlated with response to treatment (PD, SD, PR *vs.* CR) using routine imaging. The absolute numbers of ctDNA fragments (DNA copies/ml) measured by dPCR correlated with response status ($\rho = 0.3939$; $p < 0.0001$; Fig. 2*e*). Correlation of disease activity and MAF showed similar results ($\rho = 0.392$; $p < 0.001$; Fig. 2*f*). In patients with detectable cfDNA at baseline, the correlation was stronger ($\rho = 0.521$; $p < 0.001$). Specificity of dPCR regarding the detection of progression was 79.2% and sensitivity 55.2% (Supporting Information Fig. S2). Comparing active disease—defined as PR, SD or PD—*vs.* CR, specificity was 96% and sensitivity 44.7% (Supporting Information Fig. S2).

With L-PCR, specificity was (71.1%), similar to dPCR with lower sensitivity (28.6%). Comparing active disease *vs.* CR, specificity was 75% and sensitivity 29.7%. Regarding patients with positive ctDNA levels at baseline, L-PCR MAF correlated with disease activity ($\rho = 0.362$; $p = 0.004$). When data from patients with negative baseline samples were included, the strength of correlation decreased ($\rho = 0.0962$; $p = 0.0318$; Supporting Information Figs. S1*c* and S1*d*).

In summary, ctDNA was correlated with response to treatment, and dPCR displayed superior sensitivity and specificity to detect progression and to discriminate CR from active disease.

CtDNA values reflect individual disease courses

As demonstrated above, the amount of ctDNA reflected tumor mass and disease activity at individual timepoints. Furthermore, we were interested in whether individual disease monitoring using ctDNA is feasible. Therefore, the course of disease and the corresponding ctDNA values were analyzed in detail (Fig. 3*a*, Supporting Information Fig. S3 and Table S4).

Patient #6 (Fig. 3*a*) received adjuvant imatinib after initial surgery of a gastric GIST. Before inclusion, the patient experienced a relapse with peritoneal metastatic lesions. At baseline, mutated ctDNA was high (135.5 copies/ml, MAF 6.7%). Treatment with sunitinib was initiated. Mutant ctDNA copies and MAF values decreased and the patient achieved a partial response. However, ctDNA remained detectable and increased while the disease progressed again (Fig. 3*a*, Supporting Information Table S4). Patient #16 (Fig. 3*b*, Supporting Information Table S4) was included with metastatic GIST of the rectum. The patient received imatinib and ctDNA copies and MAF decreased. At day 183 ctDNA values increased while routine imaging indicated stable disease according to RECIST (Fig. 3*b*). Retrospective analysis of imaging data revealed a new, small (8 × 4 mm), contrast-enhanced lesion visible in the CT scan at Day 183 (Fig. 3*b*, red arrow) suspicious for a metastatic lesion. While receiving continued imatinib treatment the lesion disappeared and the ctDNA values decreased. From Day 358, ctDNA levels increased and preceded disease progression at Day 566. In Patient #25, ctDNA levels indicated increase of disease activity during the course of the study that was missed by imaging (Supporting Information Fig. S3A). In Patient #5 (Fig. 3*c*), two different mutations were monitored. At initial diagnosis, only a *cKIT* exon 11 mutation was detected. At study baseline (progression after imatinib and sunitinib treatment), an additional *cKIT* exon 17 mutation was identified in a surgical specimen of the small intestine, in addition to the previously reported *cKIT* exon 11 mutation. During nilotinib treatment, *cKIT* exon 11 mutated ctDNA remained stable at a low level (Fig. 3*c*, left and middle panel) while ctDNA specific for the *cKIT* exon 17 mutation increased over time and imaging demonstrated progression (Fig. 3*c*, right panel). During treatment with masitinib after Day 240, the exon 17 mutation decreased to no detectable levels, while exon 11 mutated copies massively increased in line with massive progression at Day 359. Interestingly, *cKIT* exon 17 mutation was detected by L-PCR, whereas the *cKIT* exon 11 mutation was detected by dPCR and by L-PCR only at the last visit. In Patient #3, ctDNA values significantly decreased under masitinib treatment (Supporting Information Fig. S3B). However, during the course of the disease, ctDNA values increased again despite ongoing partial response with imaging. After the end of the study, the patient experienced fulminant progression.

Thus, ctDNA monitoring might allow sensitive response monitoring especially in patients achieving stable disease and partial response as assessed by routine imaging, and might indicate increase of disease activity that precedes disease progression detected by imaging.

Successful monitoring of patients with ongoing complete response

In the intention-to-treat population, five patients achieved ongoing CR after initial surgery (Fig. 4). At baseline, ctDNA was detectable in all cases. After surgery, the amount of ctDNA dropped rapidly and all five patients showed ongoing responses during a follow-up of 62–78 months (Fig. 4). In line with the imaging result, ctDNA was not detectable during follow up, with the exception of one outlier in Patient #1. For Patient #9, the individual course of disease is shown in detail including images of the CT scans (Fig. 4*b*).

Thus, ctDNA analysis might complement disease monitoring and in cases with initially positive ctDNA could be used to avoid redundant imaging in patients with complete response after initial surgery.

Detection of additional mutations with targeted NGS

To further validate our dPCR and L-PCR data and to detect additional aberrations, we performed targeted NGS using a custom panel of 18 genes including *cKIT* and *PDGFRA* (see Materials and Methods). Using diluted sheared genomic DNA and a commercial cell-free DNA reference standard set, we were able to detect mutations with allelic frequencies down to 0.1% with our custom targeted NGS panel (data not shown). We performed targeted NGS in four patients with a total of 13 samples. Hereof, one patient was first diagnosed with metastatic GIST at baseline (#3) and three patients had a progressive disease under therapy (#6, #16 and #25). The three latter patients were pretreated with

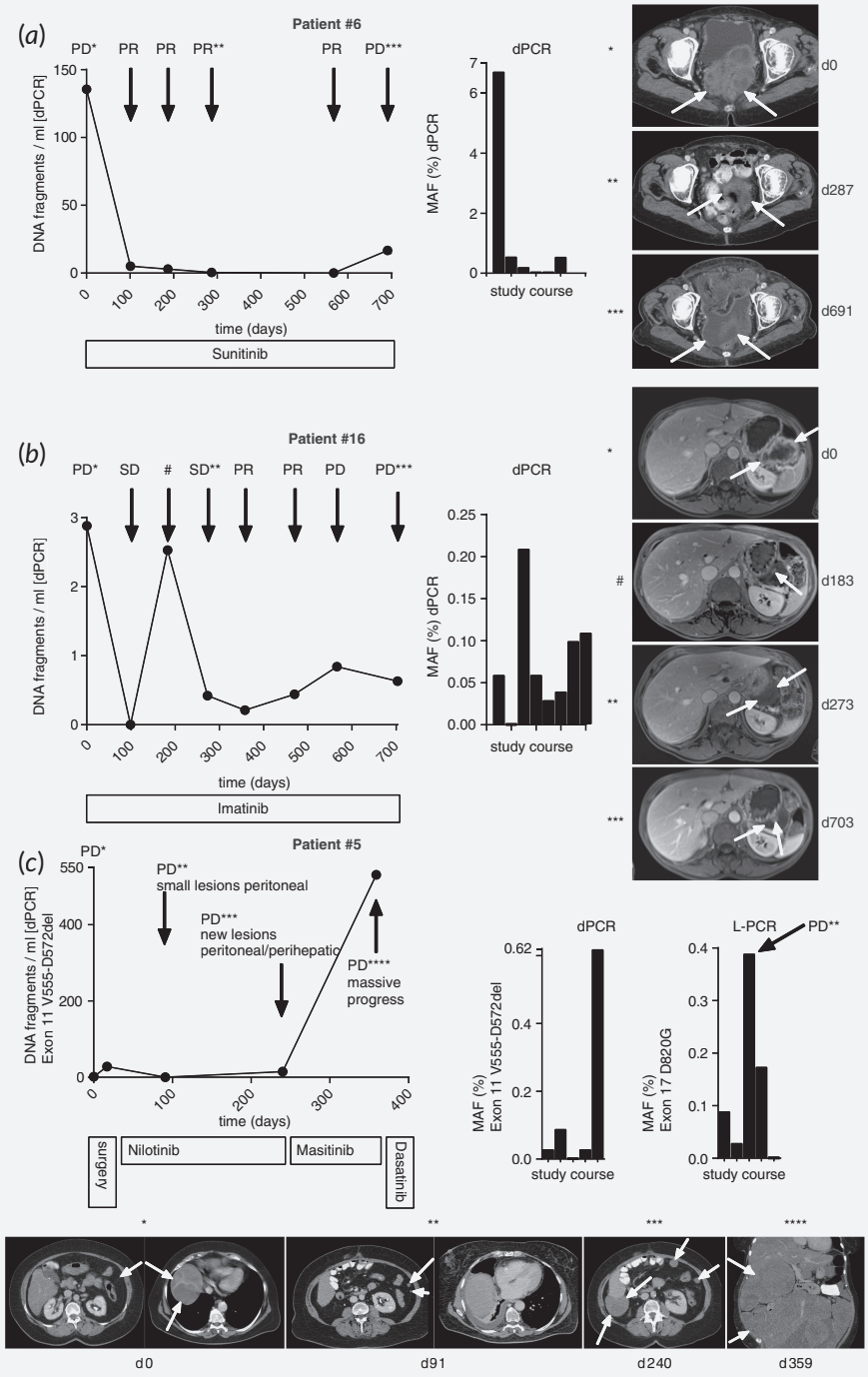

Figure 3. CtDNA values reflect individual courses of disease. Shown are the individual courses of disease, treatment history, starting at baseline (day 0) and ctDNA values in three GIST patients. The absolute numbers of ctDNA fragments per milliliter plasma of each sample are correlated to disease state as indicated (PD, progressive disease; SD, stable disease; PR, partial response). MAF (% total) measured during the course of the study is added in a separate graph. Representative CT images are shown and linked to individual timepoints by asterisks. # marks timepoints where additional analyses were performed using targeted next-generation sequencing. (*a*) Patient #6 underwent surgery at Day 567 and had progressive peritoneal lesions under imatinib treatment. Treatment was switched to sunitinib and the patient achieved partial response. (*b*) Patient #16 had PD 4343 days after initial surgery. At Day 183, imaging showed a new, contrast-enhanced lesion (red arrow) that disappeared in the subsequent CT scan at Day 273. Due to its small size, disease was classified as SD at this timepoint. (*c*) Patient #5 underwent surgery at Day 2,251 and received imatinib and sunitinib. Despite treatment the disease progressed and the patient underwent surgery again (baseline), followed by treatment with nilotinib, masitinib and dasatinib.

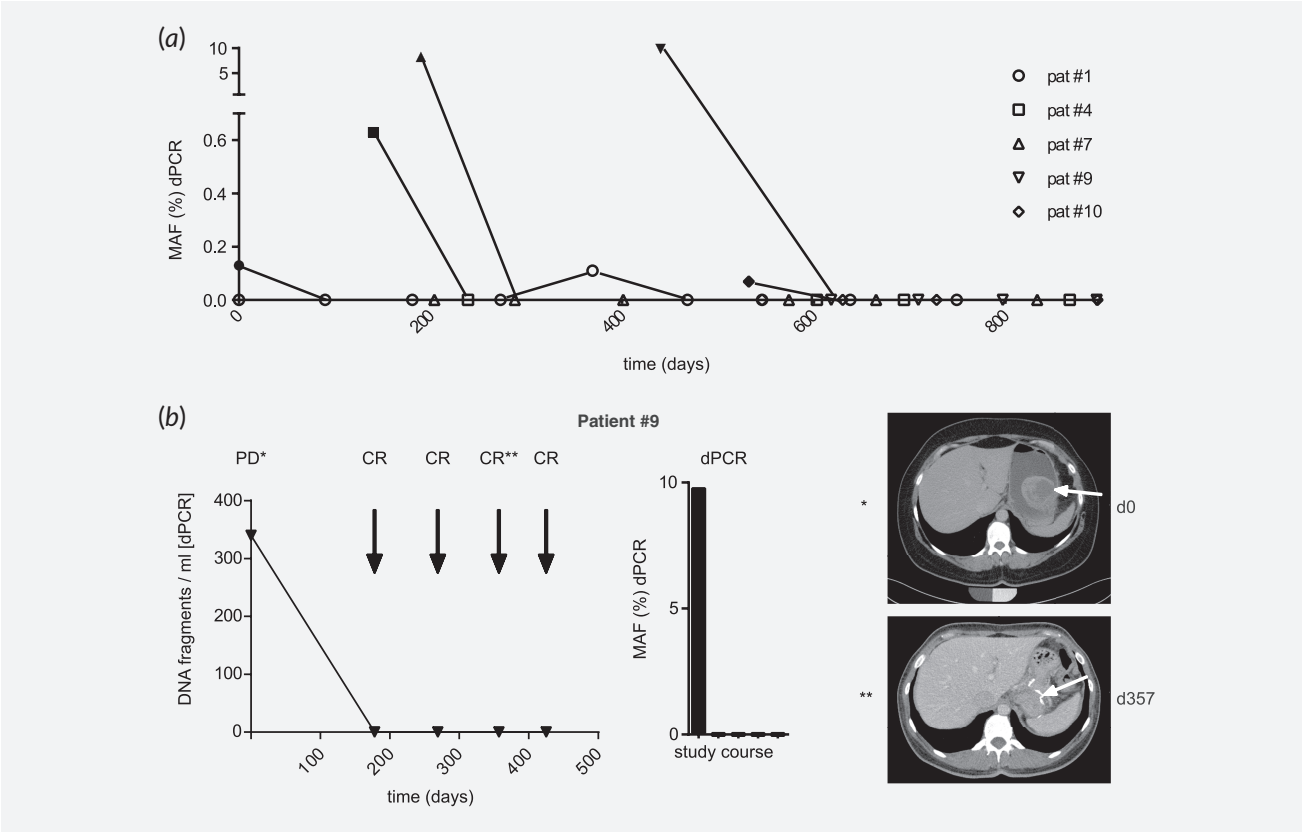

Figure 4. Long term follow-up of patients with complete response. (*a*) Shown are the ctDNA levels of five individual GIST patients that underwent surgery at baseline and achieved CR. No disease progression was observed in the follow-up period of at least 2 years. MAF (% total) measured by dPCR as indicated. All cases showed ongoing CR over an observation period of 62–78 months. Panel *b* shows the individual course of disease and the ctDNA values of one representative GIST patient that achieved CR after surgery. The absolute numbers of ctDNA fragments/ml plasma of each sample are correlated to disease state as indicated (PD, progressive disease; CR, complete response). MAF (% total) measured during the course of the study is added in a separate graph. Representative CT images are shown and linked to individual timepoints by asterisks. The red arrow at d357 indicates full resolution of previous gastric GIST.

at least one TKI. Timepoints with additional NGS analysis are marked with a pound (#) in Figure 3 and Supporting Information Figure S3. In two out of four patients (# 6 and #25), the previously described *cKIT* mutations (Exon 11 Y553-Q556del and del557-558 respectively) were detectable by NGS (Supporting Information Table S5). Of note, additional aberrations were detected in all patients. In addition to the primary *cKIT* exon 11 Y553-Q556del, a *cKIT* exon 13 V654A mutation that is known to confer imatinib resistance,[18] was found in Patient #6 at baseline and during follow-up after pretreatment with imatinib and switch to sunitinib. The same *cKIT* exon 13 V654A resistance mutation was found in Patient #25 together with an additional *cKIT* exon 17 mutation D820Y, with increasing allelic frequencies under treatment with regorafenib. The *cKIT* D820Y exchange is also well documented to cooccur with treatment resistance.[19] Furthermore, additional mutations were detected including aberrations in *TP53* and additional driver mutations in *NRAS, KRAS, HRAS, PIK3CA and BRAF* (Supporting Information Table S5).

Thus, although sensitivity of targeted NGS might be inferior to dPCR and L-PCR, NGS analysis detected additional mutations that might have contributed to disease progression and treatment resistance in all cases.

Discussion

Detection and quantitation of somatic tumor mutations in ctDNA has become a promising strategy for noninvasive monitoring of cancer.[20,21] Monitoring of ctDNA is not only a powerful technique for controlling treatment response but it also depicts evolution of the tumor genome toward acquisition of mutations associated with treatment resistance.[21,22] The amount of detectable ctDNA varies between tumor entities and is influenced by tumor burden and cell turnover.[20] Detection of low amounts of ctDNA at an early stage of the disease is challenging. For lung cancer, commercial kits are available for detecting *EGFR* mutations in ctDNA to select patients with NSCLC for the appropriate *EGFR*-directed therapy.

Monitoring in GIST is hampered by a lack of protein biomarkers and only limited sensitivity and specificity of standard imaging techniques.[13–15] However, long-term follow up is a critical part of the daily clinical routine as TKI therapy has significantly

improved the outcome in the adjuvant and palliative treatment setting.[6] Nevertheless, the optimal follow-up schedules are not known and repetitive imaging over the years is recommended in national and international guidelines for follow-up and response monitoring.

GIST tumors are a promising target for a liquid biopsy-based treatment stratification since 85–90% of the tumors carry well-characterized mutations of *cKIT* and *PDGFRA*.[23] As proof of principle, we have demonstrated before that (L-)PCR is a feasible approach to detect ctDNA in the plasma of patients with active GIST.[17] However, sensitivity and specificity of this technique are limited. We hypothesized that digital droplet PCR will display increased signal-to-noise ratio, high analytical sensitivity and high diagnostic specificity while allowing fast sample turnover at limited assay costs. Furthermore, dPCR directly provides ctDNA quantification without the need of DNA preamplification or calibration as for real-time PCR with L-PCR. Previous approaches had shown promising results for dPCR in a limited number of GIST patients with proven mutations in exon 11.[24]

We analyzed 156 plasma samples prospectively collected from 25 patients with active GIST for tumor-specific *cKIT* and *PDGFR* mutations known from individual tissue analysis. Combined use of L-PCR and dPCR detected ctDNA in 92% of these patients. Using a single diagnostic approach, dPCR showed a higher specificity (79% *vs.* 71.1%) and sensitivity (55% *vs.* 26.8%) for detecting ctDNA in GIST patients compared to L-PCR (Supporting Information Fig. S2). In our previously published data set using L-PCR, ctDNA was detectable in 15 out of 38 GIST patients (40%) or in 9 of 18 patients (50%) with active disease.[17]

This is in line with previously published data confirming the clinical utility and high diagnostic specificity of dPCR in detection of KRAS mutations in ctDNA in patients with colorectal cancer.[25] Our data clearly demonstrate that ctDNA analysis recapitulates *cKIT* and *PDGFRA* mutations derived from tumor cells and reflects amount of disease and response to treatment. These data strengthen the high diagnostic potential of ctDNA analysis in patients with GIST harboring a *cKIT* or *PDGFRA* mutation.

In our previous approach using L-PCR, ctDNA was not detectable in individuals with active disease showing response receiving TKI.[17] By combining L-PCR with dPCR in the current approach, all individuals achieving PR under TKI treatment still showed detectable ctDNA levels despite response. Furthermore, ctDNA was detectable in 7 out of 8 patients (87.5%) with localized disease. In contrast, Boonstra *et al.*[24] used a *cKIT* ex 11 drop-off probe based dPCR assay resulting in a detection rate of 93% in metastatic GIST but only 12.5% for patients with localized disease. However, differences in tumor size and localization might contribute to the discrepant findings.

Patients achieving CR after surgery would probably benefit the most from a reduced number of scans. In our cohort, no post-surgery patient with CR had detectable ctDNA using dPCR at the first study visit postintervention, resulting in a false-positive detection rate of 0%. Analyzing the entire follow-up period, only one single value in one patient was low-level positive resulting in a false positive detection rate of 3.58%. None of these patients relapsed during follow-up and no patient progressed in the optional poststudy follow-up allowing an analysis of up to 78 months. In contrast, the false positive detection rate in our previous cohort was 30% using L-PCR only.[17] We therefore conclude that monitoring patients, achieving CR postsurgery, by dPCR is a valid and feasible approach.

Analysis of ctDNA has detected cancer mutations that were missed in corresponding tissue specimen and thus can provide information about clonal and subclonal mutations.[22,24,26,27] It has been shown that in GIST the clonal genetic composition changes over time and secondary mutations causing treatment resistance can be detected in tissue[28,29] and plasma samples of patients with progression.[17,30] Accordingly, in Patient #5, L-PCR detected a *cKIT* exon 17 D820G mutation known to mediate imatinib resistance in ctDNA,[28] in addition to the preexistent *cKIT* exon 11 mutation, reflecting selection of a treatment-resistant disease clone contributing to subsequent progression. Targeted NGS of ctDNA offers the advantage of covering hundreds to thousands of amplicons in one assay read in an unbiased fashion.[31,32] NGS was shown to successfully detect ctDNA in plasma,[30,33–36] and in single cases to capture clonal heterogeneity in GIST patients.[30,34,35] However, GIST liquid biopsy studies that used NGS had either low patient numbers[34,35] or were limited to localized disease,[36] and data showing a long-term follow up of individual GIST patients are lacking. Recently, Namlos *et al.* showed that detection of ctDNA in plasma of GIST patients using NGS correlated with high tumor burden but at a relevantly low ctDNA detection rate (19 of 50 patients, i.e., 38%).[30] Similarly, Xu *et al.* detected ctDNA in 56.3% of GIST patients when applying NGS, mainly investigating patients with larger tumors.[33] In line with these data, using targeted NGS, we detected the primary *cKIT* mutation only in two out of four patients, in which detection by dPCR was feasible. However, serial NGS analysis documented selection of additional *cKIT* mutations (*cKIT* V654A, D820Y) that are known to mediate imatinib resistance in two patients.[18,19] In Patient #25, increasing allelic frequencies of these two resistance mutations demonstrated selection during treatment. Of note, serial analysis also recovered *TP53* mutations in three patients and additional driver mutations in all four patients examined with targeted NGS, including mutations in *PIK3CA, N/H/KRAS* and *BRAF*, *PTEN* and *CTNNB1*. For Patient #3 several additional mutations (*BRAF* V600E, *NRAS* and *PI3KCA*) were detected already at baseline, indicating genetic heterogeneity was present already at baseline. *CTNNB1* mutations have been described in patients with GIST and cooccurring desmoid tumors.[37] However, our patient had no history or evidence of cooccurring desmoid. PTEN deficiency has been described in the context of imatinib resistance.[38] The prognostic or predictive significance of *TP53* mutations in GIST patients is currently unclear.[39] However, additional driver mutations are known from previous studies in GIST.[40–42] Although the prognostic and predictive significance of additional driver mutations in GIST is unknown, selection of driver mutations might cause treatment resistance to *cKIT* and *PDGFRA* inhibitors and might indicate

alternative treatment options if druggable activating mutations are detected.

NGS is time-consuming, requires a rather high amount of input ctDNA and demands extensive bioinformatic analyses (data polishing) to achieve a high diagnostic sensitivity and specificity, respectively.[43] dPCR can simultaneously detect up to four different mutations.[25] Thus, dPCR might be most suitable as a robust and sensitive point-of-care platform for the detection and monitoring of nonsynonymous stereotypic mutations.[21] In contrast, NGS might be used in previously treated patients to guide further therapy.

Limitations of our study include small sample size. Thus, it does not allow definitive conclusions to be drawn regarding sensitivity and specificity for detecting relapse and progression. Assessment of ctDNA should therefore be incorporated as companion biomarker in future prospective trials. The mitotic index was also suspected to affect ctDNA levels and thus the detection rate. However, we did not find a clear correlation between mitotic index and amount of ctDNA levels. Two patients with 12 cm and 31 cm sized gastric GIST and a mitotic index of 4/50 HPF each displayed ctDNA MAF of 0.069% (Patient #10) and 12.43% (Patient #11, Supporting Information Table S4), respectively. Additional biologic properties might affect release of ctDNA in individual patients. This includes biological features like tumor size, location and vascularization.[26] A larger number of patients will be necessary to define criteria and to identify specific subgroups of GIST patients that are especially eligible for monitoring by ctDNA.

Positivity for ctDNA at baseline in patients with measurable disease seems to be mandatory to complement or even replace imaging. Thus, future efforts must focus on developing ctDNA detection assays with a sensitivity of ideally 100% without increasing false positive rates. Standardization of the technique will also be critical to harmonize national or international efforts in an academic setting. CtDNA has a short half-life of less than 2 hr.[44] In our study, blood samples were processed within 4 hr after withdrawal. We can therefore not exclude beginning degradation of cfDNA in a subset of samples. Standards for preanalytical and analytical conditions will be essential to obtain robust and reproducible results. In addition, the short half-life of ctDNA explains that none of the analyzed patients analyzed in this study showed a transient increase of tumor-specific *cKIT* or *PDGFRA* ctDNA in the plasma (tumor flare) after starting medical treatment. Whether sampling within hours or days after institution of treatment would allow to capture a ctDNA flare and whether a ctDNA flare adds additional predictive or prognostic information remains to be demonstrated.

Taken together, dPCR and L-PCR allow detection of somatic tumor mutations in ctDNA of patients with GIST. The amount of mutated ctDNA reflects tumor burden and disease activity and can be used for monitoring treatment response and follow-up after surgery. CtDNA monitoring may complement standard of care imaging especially in patients where standard imaging reveals unclear changes of tumor volume. In patients with CR after initial surgery, repetitive imaging might be reduced. Dynamic ctDNA monitoring in GIST should include assays detecting variants often associated with treatment resistance in order to detect patients at risk for subsequent progression, including exchanges in *cKIT* exon 13 (V654A), exon 14 (T670I), exon 17 and *PDGFR* D842V.[18,28] NGS will allow detection of additional mutations that might indicate disease progression, including driver mutations (*BRAF*, *NRAS*, *PIK3CA*, *PTEN* and *CTNNB1*) that might guide further treatment. Future prospective trials in GIST should incorporate multiplex ctDNA analysis covering individual primary and frequently observed secondary resistance mutations as companion biomarker to determine the significance of ctDNA with respect to clinical endpoints in larger patient cohorts to improve treatment monitoring and to guide adjuvant treatment.

Acknowledgements

The authors would also like to acknowledge the support of the Munich Study Center, the University of Freiburg Medical Faculty, the Comprehensive Cancer Center Freiburg (CCCF), the German Cancer Consortium (DKTK; grant no. L665 to NvB), the Bundesministerium für Bildung und Forschung (BMBF; grant no. 13GW0198E to NvB) and Novartis Germany for research support (study no. CSTI5781BDE78T to NvB). We thank Folker Schneller for patient management, Sandra Eckert and Monika Mathew for administrative support, and Amanda Kalman for critical advice. In addition, the authors want to thank Laura-Jane Behl as well as the whole "Genomics and Proteomics Core Facility of the DKFZ Heidelberg (Germany)" for providing excellent sequencing service.

References

1. Hohenberger P, Reichardt P, Gebauer B, et al. Gastrointestinal stromal tumors (GIST)—current concepts of surgical management. *Dtsch Med Wochenschr* 2004;129:1817–20.
2. Reichardt P, Pink D, Mrozek A, et al. Gastrointestinal stromal tumors (GIST). *Z Gastroenterol* 2004;42:327–31.
3. Casali PG, Jost L, Reichardt P, et al. Gastrointestinal stromal tumors: ESMO clinical recommendations for diagnosis, treatment and follow-up. *Ann Oncol* 2008;19(Suppl 2):ii35–8.
4. (MetaGIST) GSTM-AG. Comparison of two doses of imatinib for the treatment of unresectable or metastatic gastrointestinal stromal tumors: a meta-analysis of 1,640 patients. *J Clin Oncol* 2010;28:1247–53.
5. von Mehren M, Heinrich MC, Joensuu H, et al. Follow-up results after 9 years (yrs) of the ongoing, phase II B2222 trial of imatinib mesylate (IM) in patients (pts) with metastatic or unresectable KIT+ gastrointestinal stromal tumors (GIST) 2011 *ASCO Annual Meeting. J Clin Oncol* 2011;29:abstr10016.
6. von Mehren M, Joensuu H. Gastrointestinal stromal tumors. *J Clin Oncol* 2018;36:136–43.
7. Demetri GD, van Oosterom AT, Garrett CR, et al. Efficacy and safety of sunitinib in patients with advanced gastrointestinal stromal tumour after failure of imatinib: a randomised controlled trial. *Lancet* 2006;368:1329–38.
8. Joensuu H, Vehtari A, Riihimaki J, et al. Risk of recurrence of gastrointestinal stromal tumour after surgery: an analysis of pooled population-based cohorts. *Lancet Oncol* 2012;13:265–74.
9. Joensuu H. Risk stratification of patients diagnosed with gastrointestinal stromal tumor. *Hum Pathol* 2008;39:1411–9.
10. Miettinen M, Lasota J. Gastrointestinal stromal tumors: pathology and prognosis at different sites. *Semin Diagn Pathol* 2006;23:70–83.
11. Joensuu H, Rutkowski P, Nishida T, et al. KIT and PDGFRA mutations and the risk of GI stromal tumor recurrence. *J Clin Oncol* 2015;33:634–42.
12. Joensuu H, Eriksson M, Sundby Hall K, et al. One vs three years of adjuvant imatinib for operable gastrointestinal stromal tumor: a randomized trial. *JAMA* 2012;307:1265–72.

13. Antoch G, Herrmann K, Heusner TA, et al. Imaging procedures for gastrointestinal stromal tumors. *Radiologe* 2009;49:1109–16.
14. Antoch G, Kanja J, Bauer S, et al. Comparison of PET, CT, and dual-modality PET/CT imaging for monitoring of imatinib (STI571) therapy in patients with gastrointestinal stromal tumors. *J Nucl Med* 2004;45:357–65.
15. Gambhir SS, Czernin J, Schwimmer J, et al. A tabulated summary of the FDG PET literature. *J Nucl Med* 2001;42:1S–93S.
16. Hirota S, Isozaki K, Moriyama Y, et al. Gain-of-function mutations of c-kit in human gastrointestinal stromal tumors. *Science* 1998;279:577–80.
17. Maier J, Lange T, Kerle I, et al. Detection of mutant free circulating tumor DNA in the plasma of patients with gastrointestinal stromal tumor harboring activating mutations of CKIT or PDGFRA. *Clin Cancer Res* 2013;19:4854–67.
18. Debiec-Rychter M, Cools J, Dumez H, et al. Mechanisms of resistance to imatinib mesylate in gastrointestinal stromal tumors and activity of the PKC412 inhibitor against imatinib-resistant mutants. *Gastroenterology* 2005;128:270–9.
19. Antonescu CR, Besmer P, Guo T, et al. Acquired resistance to imatinib in gastrointestinal stromal tumor occurs through secondary gene mutation. *Clin Cancer Res* 2005;11:4182–90.
20. Bettegowda C, Sausen M, Leary RJ, et al. Detection of circulating tumor DNA in early- and late-stage human malignancies. *Sci Transl Med* 2014;6:224ra24.
21. von Bubnoff N. Liquid biopsy: approaches to dynamic genotyping in cancer. *Oncol Res Treat* 2017;40:409–16.
22. Siravegna G, Mussolin B, Buscarino M, et al. Clonal evolution and resistance to EGFR blockade in the blood of colorectal cancer patients. *Nat Med* 2015;21:827.
23. Corless CL, Barnett CM, Heinrich MC. Gastrointestinal stromal tumours: origin and molecular oncology. *Nat Rev Cancer* 2011;11:865–78.
24. Boonstra PA, Ter Elst A, Tibbesma M, et al. A single digital droplet PCR assay to detect multiple KIT exon 11 mutations in tumor and plasma from patients with gastrointestinal stromal tumors. *Oncotarget* 2018;9:13870–83.
25. Taly V, Pekin D, Benhaim L, et al. Multiplex picodroplet digital PCR to detect KRAS mutations in circulating DNA from the plasma of colorectal cancer patients. *Clin Chem* 2013;59:1722–31.
26. Jamal-Hanjani M, Wilson GA, Horswell S, et al. Detection of ubiquitous and heterogeneous mutations in cell-free DNA from patients with early-stage non-small-cell lung cancer. *Ann Oncol* 2016;27:862–7.
27. Oxnard GR, Thress KS, Alden RS, et al. Association between plasma genotyping and outcomes of treatment with Osimertinib (AZD9291) in advanced non-small-cell lung cancer. *J Clin Oncol* 2016;34:3375–82.
28. Heinrich MC, Maki RG, Corless CL, et al. Primary and secondary kinase genotypes correlate with the biological and clinical activity of sunitinib in imatinib-resistant gastrointestinal stromal tumor. *J Clin Oncol* 2008;26:5352–9.
29. Wardelmann E, Merkelbach-Bruse S, Pauls K, et al. Polyclonal evolution of multiple secondary KIT mutations in gastrointestinal stromal tumors under treatment with imatinib mesylate. *Clin Cancer Res* 2006;12:1743–9.
30. Namlos HM, Boye K, Mishkin SJ, et al. Noninvasive detection of ctDNA reveals intratumor heterogeneity and is associated with tumor burden in gastrointestinal stromal tumor. *Mol Cancer Ther* 2018;17:2473–80.
31. Newman AM, Bratman SV, To J, et al. An ultrasensitive method for quantitating circulating tumor DNA with broad patient coverage. *Nat Med* 2014;20:548–54.
32. Kinde I, Wu J, Papadopoulos N, et al. Detection and quantification of rare mutations with massively parallel sequencing. *Proc Natl Acad Sci USA* 2011;108:9530–5.
33. Xu H, Chen L, Shao Y, et al. Clinical application of circulating tumor DNA in the genetic analysis of patients with advanced GIST. *Mol Cancer Ther* 2018;17:290–6.
34. Wada N, Kurokawa Y, Takahashi T, et al. Detecting secondary C-KIT mutations in the peripheral blood of patients with Imatinib-resistant gastrointestinal stromal tumor. *Oncology* 2016;90:112–7.
35. Kang G, Bae BN, Sohn BS, et al. Detection of KIT and PDGFRA mutations in the plasma of patients with gastrointestinal stromal tumor. *Target Oncol* 2015;10:597–601.
36. Kang G, Sohn BS, Pyo JS, et al. Detecting primary KIT mutations in presurgical plasma of patients with gastrointestinal stromal tumor. *Mol Diagn Ther* 2016;20:347–51.
37. Dumont AG, Rink L, Godwin AK, et al. A non-random association of gastrointestinal stromal tumor (GIST) and desmoid tumor (deep fibromatosis): case series of 28 patients. *Ann Oncol* 2012;23:1335–40.
38. Quattrone A, Wozniak A, Dewaele B, et al. Frequent mono-allelic loss associated with deficient PTEN expression in imatinib-resistant gastrointestinal stromal tumors. *Mod Pathol* 2014;27:1510–20.
39. Ihle MA, Huss S, Jeske W, et al. Expression of cell cycle regulators and frequency of TP53 mutations in high risk gastrointestinal stromal tumors prior to adjuvant imatinib treatment. *PLoS One* 2018;13:e0193048.
40. Boikos SA, Pappo AS, Killian JK, et al. Molecular subtypes of KIT/PDGFRA wild-type gastrointestinal stromal tumors: a report from the National Institutes of Health gastrointestinal stromal tumor clinic. *JAMA Oncol* 2016;2:922–8.
41. Chen Q, Li R, Zhang ZG, et al. Oncogene mutational analysis in Chinese gastrointestinal stromal tumor patients. *Onco Targets Ther* 2018;11:2279–86.
42. Serrano C, Wang Y, Marino-Enriquez A, et al. KRAS and KIT gatekeeper mutations confer polyclonal primary Imatinib resistance in GI stromal tumors: relevance of concomitant phosphatidylinositol 3-kinase/AKT dysregulation. *J Clin Oncol* 2015;33:e93–6.
43. Newman AM, Lovejoy AF, Klass DM, et al. Integrated digital error suppression for improved detection of circulating tumor DNA. *Nat Biotechnol* 2016;34:547–55.
44. Diehl F, Schmidt K, Choti MA, et al. Circulating mutant DNA to assess tumor dynamics. *Nat Med* 2008;14:985–90.